SUPPORTING MATERIAL

SUPPLEMENTARY TEXT S1

Here we explore the kinetic scheme adapted from references (1, 2) and represented in Fig. 4*b* of the main manuscript. We reproduced it below for clarity. This scheme is based on the requirement for an enzyme to adopt two mutually conformations to achieve two distinct steps during catalysis. When adapted to the CPR, the NADPH-based FAD-mediated reduction of FMN is supposed to occur in the locked state (L) where the two flavins are in short distance whereas the external electron transfer (ET) to the final substrate is supposed to occur in the unlocked state (U) where the FMN is exposed to solvent.

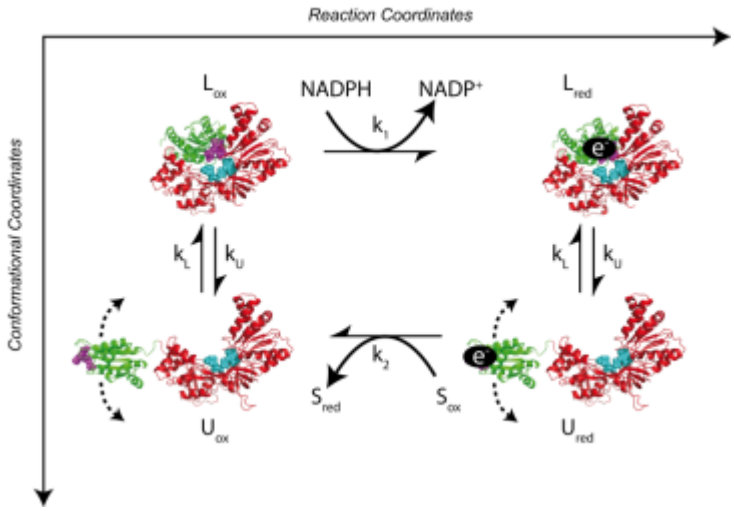

Kinetic scheme linking two conformational states of CPR and their respective catalytic steps where the conformational equilibrium is not altered by chemical transformations.

In this model, the enzyme is assumed to sample the locked (L) and unlocked (U) conformational states with closure (k_L) and opening (k_U) rates that are insensitive to the protein oxidation state. The equilibrium constant K_e is defined as $k_U / k_L = p_U / p_L$ where p_U and p_L are the relative populations of the unlocked and locked states, respectively ($p_U + p_L = 1$). All other chemical events, including substrate binding, chemical transformations and product release are incorporated into the k_1 and k_2 rates that describe the CPR reduction/oxidation cycle. The k_1 rate constant describes the NADPH binding step to the oxidized locked conformation (L_{ox}), the hydride transfer from NADPH to FAD, the release of $NADP^+$, and the interflavin electron transfer, resulting in the reduced locked state (L_{red}) and the oxidized $NADP^+$. The k_2 rate constant describes the binding of the oxidized substrate (S_{ox}) to the FMN-reduced unlocked conformation (U_{red}), the intermolecular ET and the release of the reduced substrate (S_{red}). Importantly, this mechanism does not exclude possible additional conformation changes that may occur during the chemical steps k_1 and k_2, such as local rearrangements or even domain reorientations, the only requirement being that domain relative orientations are preserved prior to and after chemical events.

In the following we provide the detailed calculation of the enzymatic turnover k_{obs}, defined as the number of substrate molecules formed by unit of time by a single CPR molecule, following the abovementioned kinetic scheme. The relationship between the enzymatic turnover, the rate of formation of the product (reduced substrate such as cytochrome *c*), and the total enzyme concentration E_T is as follows:

$$k_{obs} = \frac{1}{E_T}\frac{d[S_{red}]}{dt} \qquad \text{(Eq. 1)}$$

In order to establish the relationship between d[Sred]/dt and the kinetic parameters, we derive the following differential equations from the kinetic scheme:

$$\begin{aligned}
\frac{d[U_{ox}]}{dt} &= -k_L[U_{ox}] + k_U[L_{ox}] + k_2[U_{red}] && (a)\\
\frac{d[L_{ox}]}{dt} &= k_L[U_{ox}] - (k_U + k_1[L_{ox}]) && (b)\\
\frac{d[L_{red}]}{dt} &= k_1[L_{ox}] + k_L[U_{red}] - k_U[L_{red}] && (c)\\
\frac{d[U_{red}]}{dt} &= k_U[L_{red}] - (k_L + k_2[U_{red}]) && (d)
\end{aligned} \qquad \text{(Eq. 2)}$$

Under stationary conditions, the time-dependent derivatives vanish and the relationships between the steady-state concentrations of the various species can be determined to:

$$\begin{aligned}
[U_{ox}] &= \frac{(k_U + k_1)}{k_L}\frac{k_2}{k_1}[U_{red}] && (a)\\
[L_{ox}] &= \frac{k_2}{k_1}[U_{red}] && (b)\\
[L_{red}] &= \frac{(k_L + k_2)}{k_U}[U_{red}] && (c)
\end{aligned} \qquad \text{(Eq. 3)}$$

Reminding that the total concentration of the enzyme [E_T] is constant, we obtain:

$$E_T = [U_{ox}] + [L_{ox}] + [L_{red}] + [U_{red}] \qquad \text{(Eq. 4)}$$

By combining Eq. 3 and Eq. 4, we derive the rate of formation of the reduced substrate:

$$\frac{d[S_{red}]}{dt} = k_2[U_{red}] = \frac{k_U k_L}{(k_U + k_L)}\frac{k_1 k_2 [E_T]}{(k_U k_2 + k_1 k_2 + k_L k_1)} \qquad \text{(Eq. 5)}$$

The relative populations p_U and p_L are dependent on K_e and k_U and k_L parameters according to the equations:

$$p_U = 1 - p_L = \frac{K_e}{1 + K_e} = \frac{k_U}{k_U + k_L} \qquad \text{(Eq. 6)}$$

which enables us to derive the final equation for the turnover:

$$k_{obs} = \frac{p_U p_L (k_U + k_L)}{\left(1 + \frac{k_U}{k_1} + \frac{k_L}{k_2}\right)} \qquad \text{(Eq. 7)}$$

In this equation, we recognize the term $P = p_U p_L = p_U(1\text{-}p_U)$ that has a parabolic shape when P is plotted versus p_U. Under the assumption that the conformational exchange occurs on a

slower timescale than enzymatic events (i.e. $k_1 >> k_U$ and $k_2 >> k_L$), the Eq. 7 can be simplified to:

$$k_{obs} = p_U p_L (k_U + k_L) \quad \text{(Eq. 8)}$$

Under such conditions, the turnover is only controlled by the parameters k_U and k_L that define the conformational transition (i.e. rates and populations) and that are the rate-limiting steps. Notably the turnover does not depend on the k_1 and k_2 rates. In general this equation does not display a bell-shape behavior when k_{obs} is plotted versus k_U or k_L, unless the sum k_U+k_L is kept constant as proposed in (2). However this is a strong requirement on the physico-chemical properties of the system because all parameters k_U, k_L and p_U, p_L are intimately linked.
On the other hand, assuming that conformational exchange is faster than chemical events (i.e. $k_U >> k_1$ and $k_L >> k_2$), the turnover simplifies to:

$$k_{obs} = \frac{p_U p_L (k_U + k_L)}{\left(\frac{k_U}{k_L} + \frac{k_L}{k_2} \right)} \quad \text{(Eq. 9)}$$

In addition, if the condition $k=k_1=k_2$ is fulfilled, the turnover k_{obs} can be expressed as a simple form:

$$k_{obs} = p_U p_L k \quad \text{(Eq. 10)}$$

In this case, a perfectly symmetric bell-shape curve is obtained for $k_{obs}=f(p_U)$ with maximum activity for $p_U = p_L = 0.5$ (next figure, panel D), i.e. for $K_e = 1$. In the general case where $k_2 \neq k_1$, an asymmetric bell-shape curve is obtained and the relative populations for maximum activity depends on k_1 and k_2 rates (next figure, panels A-C). Based on Eq. 9, the maximum activity is obtained for

$$K_e = \sqrt{\frac{k_1}{k_2}} \quad \text{(Eq. 11)}$$

and is predicted to be:

$$(k_{obs})_{max} = \frac{k_1 k_2}{\left(\sqrt{k_1} + \sqrt{k_2} \right)^2} \quad \text{(Eq. 12)}$$

Therefore, for instance, slower k_1 rate (FMN reduction rate) and faster k_2 rate (external ET) can be compensated by increasing proportion of the locked state that is competent for FMN reduction. The main conclusion drawn from this analysis is that the assumption of fast conformational exchange results in a turnover rate of symmetric or asymmetric bell-shape curve when plotted against populations without additional constraint and that maximal activity can be obtained for a well-balanced proportion of the two conformations that are active at distinct steps of catalysis.

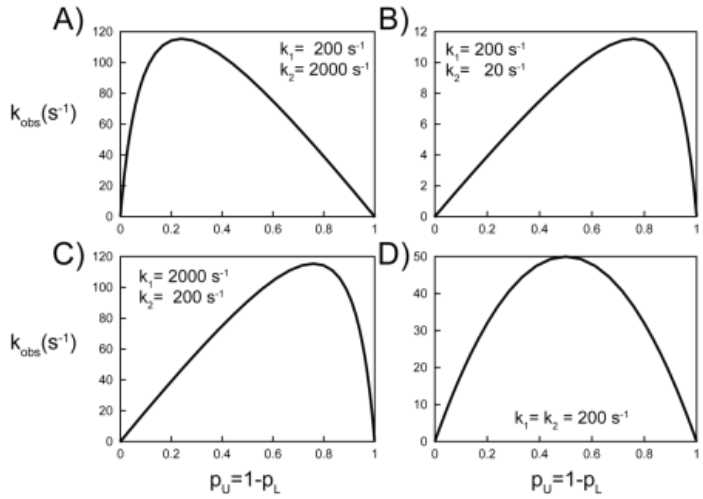

Simulation of k_{obs} using Eq. 9. Different combinations of k_1 and k_2 were used to generate the curves in panels A-B-C-D.

FIGURE S1

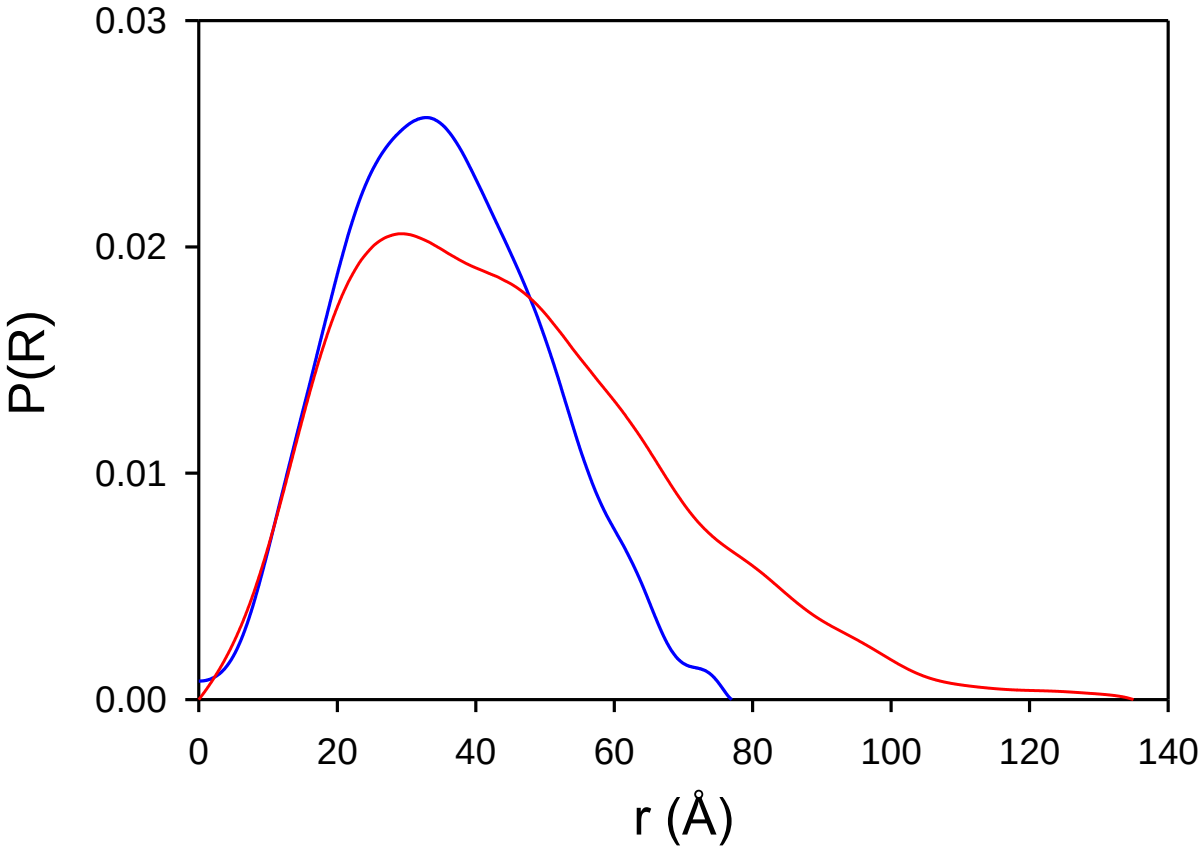

Distance distribution of human CPR observed at low and extrapolated to the higher ionic strength at pH 7.4. Pair distance distribution functions P(R) were calculated from extrapolated SAXS curves at 0 (blue) or infinite (red) ionic strength.

FIGURE S2

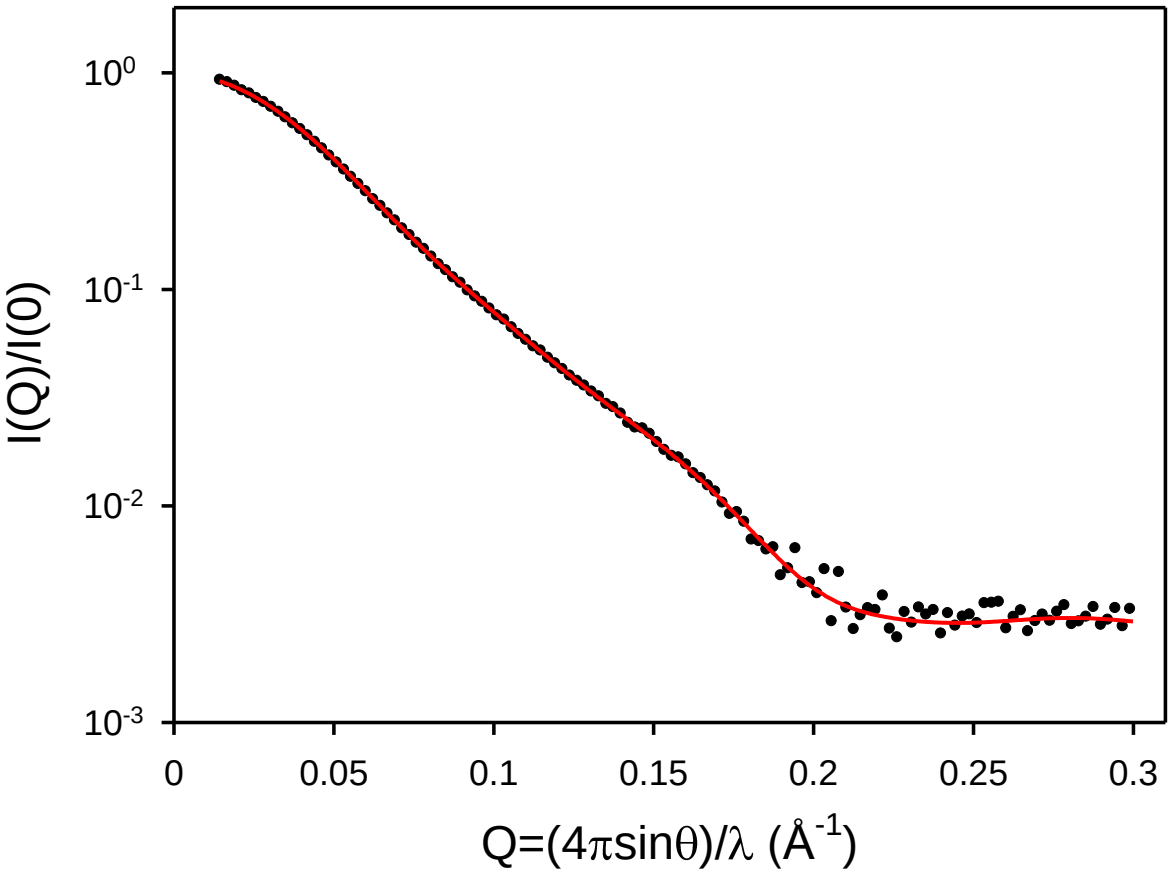

Simulation of the SAXS curve extrapolated to the higher ionic strength and associated CPR structures. The extrapolated SAXS curve is shown in black dots and the best-fit curve obtained from EOM optimization is shown in red.

FIGURE S3

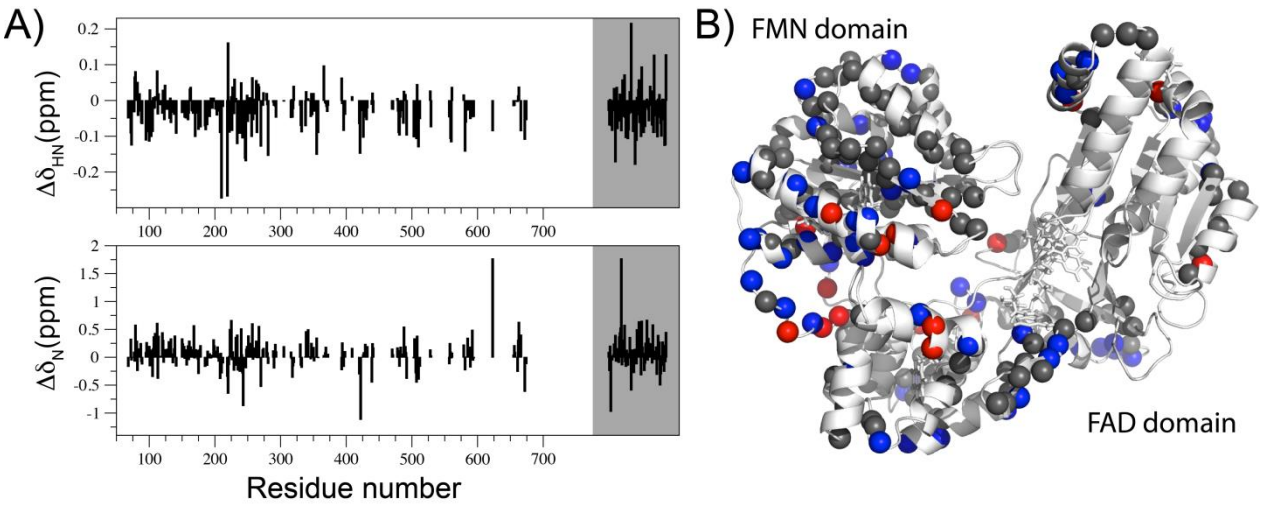

Chemical shifts variations of selected amino acids at 0 M and 1 M NaCl concentrations. A, Amide $^{1}H_N$ and ^{15}N chemical shift variation ($\Delta\delta H_N$ and $\Delta\delta_N$) versus residue number. The chemical shift variation was calculated as $\delta_1 - \delta_0$ where δ_0 and δ_1 are the chemical shifts observed at 0 and 1M salt concentration respectively. The data for unassigned crosspeaks are represented with a grey background. B, The chemical shift perturbation data are reported on the CPR closed conformation as colored spheres. The N atoms for which chemical shifts data were available are represented as spheres, with the default grey color. In blue color, residues for which ^{1}H or ^{15}N chemical shift variations were larger than one standard deviation value. Residues for which ^{1}H or ^{15}N chemical shift variations are larger than twice the deviation standard value are shown in red.

TABLE S1

		FMN domain			FAD/connecting domain		
I = 0 M	$\langle R_1 \rangle$ (s^{-1})	0.27	±	0.02	0.28	±	0.07
	$\langle R_2 \rangle$ (s^{-1})	61	±	6	61	±	8
	$\langle R_2/R_1 \rangle$	226	±	26	225	±	44
	$\langle \tau_c \rangle$ (ns)	30.3	±	1.8	30.1	±	3.3
I = 0.8 M	$\langle R_1 \rangle$ (s^{-1})	0.53	±	0.09	0.33	±	0.07
	$\langle R_2 \rangle$ (s^{-1})	31.5	±	4.5	54.8	±	13.5
	$\langle R_2/R_1 \rangle$	59.8	±	20.0	181	±	71
	$\langle \tau_c \rangle$ (ns)	15.2	±	2.6	26.6	±	5.4
I = 1 M	$\langle R_1 \rangle$ (s^{-1})	0.82	±	0.47	0.43	±	0.25
	$\langle R_2 \rangle$ (s^{-1})	23.0	±	4.6	49.8	±	14.1
	$\langle R_2/R_1 \rangle$	31.8	±	12.8	159	±	75
	$\langle \tau_c \rangle$ (ns)	11.0	±	2.0	24.8	±	2.6

Averaged NMR ^{15}N relaxation parameters and correlation times derived from the ^{15}N R_2/R_1 ratios collected at 0 M (3), 0.8 M and 1 M NaCl concentrations.

FIGURE S4

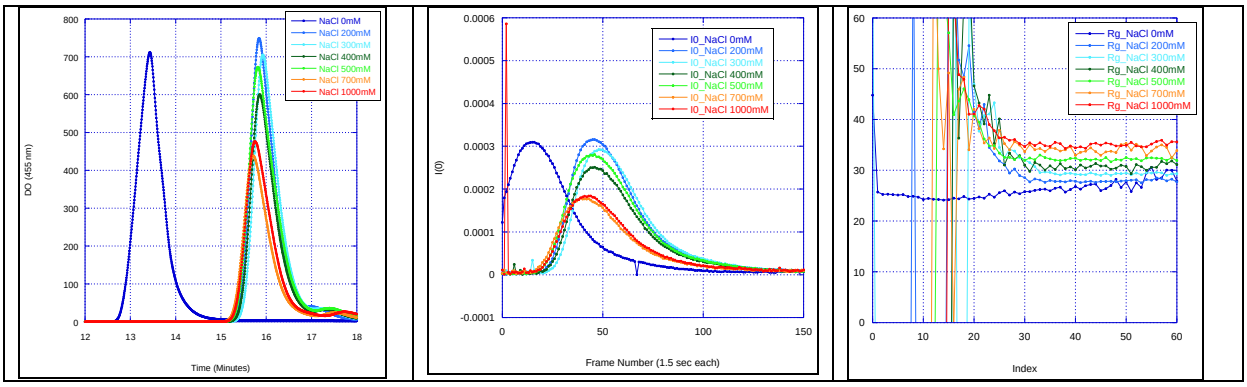

SAXS elution profiles of the CPR solutions under several salt concentrations at pH 7.4. For each condition, 50 µl of CPR at about 10 g/l were injected and flown through an Agilent Biosec3-300 SEC column at 0.2 ml/min, T=20°C. SAXS acquisition started with the same delay after injection for all the investigated conditions.

A/ The absorption at 455 nm measured before the SAXS cell, is shown as a function of time. The protein was eluted at similar times for all conditions, except for the case of no ionic strength, where unscreened intermolecular repulsion is probably the origin of the observed shift in the elution time.

B/ The I(0) values extrapolated using Guinier linearization are shown as a function of the frame number. The I(0) values closely follow the 455 nm absorption profiles, underlying the fact that the protein is a monomer in all cases.

C/ The Rg values extrapolated using Guinier linearization are shown as a function of the frame number. The large Rg values observed in the frames before the main elution peak denote the presence of a very small amount of aggregates in the injected solutions, thus justifying the use of the SEC-SAXS set-up. The existence of a plateau in the Rg profile at all conditions except at [NaCl]=0 mM clearly proves the sample monodispersity under the main elution peak, from which the SAXS curves were further selected and averaged. The Rg profile at [NaCl]=0mM displays a concentration dependent curve, with Rg values decreasing with increasing concentration. This behavior is typical of unscreened intermolecular repulsions. The small Q-range part of the final SAXS curve at [NaCl]=0 mM was therefore taken from a very low concentration frame (number 33), where intermolecular effects were negligible, and rescaled to the large Q-values part, taken from the average of the curves under the elution peak, to gain more statistics.

SUPPORTING REFERENCES

1. Haque, M. M., M. Bayachou, M. A. Fadlalla, D. Durra, and D. J. Stuehr. 2013. Charge-pairing interactions control the conformational setpoint and motions of the FMN domain in neuronal nitric oxide synthase. Biochem. J. 450:607-617.
2. Haque, M. M., C. Kenney, J. Tejero, and D. J. Stuehr. 2011. A kinetic model linking protein conformational motions, interflavin electron transfer and electron flux through a dual-flavin enzyme-simulating the reductase activity of the endothelial and neuronal nitric oxide synthase flavoprotein domains. FEBS J. 278:4055-4069.
3. Vincent, B., N. Morellet, F. Fatemi, L. Aigrain, G. Truan, E. Guittet, and E. Lescop. 2012. The closed and compact domain organization of the 70-kDa human cytochrome P450 reductase in its oxidized state as revealed by NMR. J. Mol. Biol. 420:296-309.